Progress in Oceanography
September 2015, Volume 137, Part B, Pages 484-497
http://dx.doi.org/10.1016/j.pocean.2015.04.026

Decrease in diatom palatability contributes to bloom formation in the Western English Channel

L. Polimene[a, *], A. Mitra[b], S.F. Sailley[a], S. Ciavatta[a, c], C.E. Widdicombe[a], A. Atkinson[a], J.I. Allen[a, c]

[a] Plymouth Marine Laboratory, Prospect Place, Plymouth, PL1 3DH, UK
[b] Centre for Sustainable Aquatic Research (CSAR), Swansea University, Swansea SA2 8PP, UK
[c] National Centre for Earth Observation, Plymouth Marine Laboratory, UK

*: Corresponding author : L. Polimene, email address : luca@pml.ac.uk

Abstract:

The aim of this paper is to investigate the role of phytoplankton nutritional status in the formation of the spring bloom regularly observed at the station L4 in the Western English Channel. Using a modelling approach, we tested the hypothesis that the increase in light from winter to spring induces a decrease in diatom nutritional status (i.e., an increase in the C:N and C:P ratios), thereby reducing their palatability and allowing them to bloom. To this end, a formulation describing the Stoichiometric Modulation of Predation (SMP) has been implemented in a simplified version of the European Regional Seas Ecosystem Model (ERSEM). The model was coupled with the General Ocean Turbulence Model (GOTM), implemented at the station L4 and run for 10 years (2000–2009). Simulated carbon to nutrient ratios in diatoms were analysed in relation to microzooplankton biomass, grazing and assimilation efficiency. The model reproduced *in situ* data evolutions and showed the importance of microzooplankton grazing in controlling the early onset of the bloom. Simulation results supported our hypothesis and provided a conceptual model explaining the formation of the diatom spring bloom in the investigated area. However, additional data describing the microzooplankton grazing impact and the variation of carbon to nutrient ratios inside phytoplanktonic cells are required to further validate the proposed mechanisms.

Highlights

► Abiotic and biotic mechanisms underpin bloom dynamics. ► Phytoplankton nutritional status contributes to bloom formation and evolution. ► High C:P in diatoms reduces the transfer of carbon to the higher trophic levels.

INTRODUCTION

Phytoplankton blooms are important events triggering a series of processes and trophic interactions which impact the whole marine ecosystem, from biogeochemical cycles to secondary production and fisheries (Legendre, 1990; Irigoien et al. 2005). These blooms manifest as a dramatic increase in the phytoplankton standing stock over a relatively short period of time.

Some studies have emphasised the role of the physical environment in creating the conditions required for a bloom (Huisman et al., 1999; Taylor and Ferrari 2011; Smyth et al, 2014) while others have suggested that biotic factors such as grazing and phytoplankton physiology could also play a critical role (Irigoien et al., 2005; Mitra and Flynn 2006). However, a conceptual model integrating the contribution of abiotic and biotic elements to the formation and evolution of a phytoplanktonic bloom is still lacking.

Recently, Smyth et al (2014) suggested that the air-sea heat flux play a crucial role in triggering phytoplankton blooms in the Western English Channel. By analysing historical time series data, at station L4 south of Plymouth (http://www.westernchannelobservatory.org.uk), these authors found that the beginning of the phytoplankton blooms regularly (on average by 30 days) follows the inversion of the net heat flux (NHF) into the ocean from negative to positive. Positive NHF (i.e., heat flux from atmosphere to ocean) decreases the turbulence and hence vertical mixing. This leads to an increase in the residence time of phytoplankton in the euphotic zone allowing some phytoplanktonic groups (such as diatoms) to escape grazing control and form blooms. In contrast, phytoplankton stocks are likely to be controlled by microzooplankton during winter when the NHF is negative (i.e., heat flux from ocean to atmosphere) and increase in vertical mixing prevents an adequate light exposure for growth.

All the above mentioned physical factors not only affect directly the timing and amplitude of the bloom but also have the potential to modulate biotic responses which facilitate phytoplankton growth. In particular, the increased residence time in the well-lit layer of the water column and the consequent increase in light exposure might have significant effects on the interactions between phytoplankton and grazers, potentially favouring the increase of phytoplankton biomass.

Previous laboratory and field studies have shown that under increasing light and temperature, the ratio of carbon to nutrient in phytoplankton increases (Urabe and Sterner, 1996; Hessen et al., 2002; Martiny et al., 2013) with significant consequences for the performance of grazers feeding on them (Urabe and Sterner, 1996; Hessen et al., 2002). Urabe and Sterner (1996), studying a predator-prey system comprising an alga prey consumed by a predatory zooplankton, found that (under experimental conditions) the growth of the grazer was related to the ratio between light and the limiting nutrient. Interestingly, the grazer growth rate was linearly related to the algal biomass only at low light intensity while, at increasing light levels, it started to decrease due to the decrease in the nutrient quality of the prey. This result was interpreted by invoking decoupling between photosynthesis and nutrient uptake which occurs under high light to nutrient ratio.

The cellular imbalance between carbon and nutrient made the algae less palatable for zooplankton. Unlike phytoplankton, zooplankton physiology does not allow a substantial variability of internal stoichiometry (Loladze et al., 2000, Siuda and Dam, 2010) and therefore requires nutrient rich prey to grow efficiently. Various studies have demonstrated that even small changes in phytoplankton stoichiometry can be associated with significant changes in food palatability and therefore affect zooplankton prey selection, physiological processes and thus efficiency (Flynn et al., 1996; Jones and Flynn, 2005). Loladze et al. (2000) proposed a model in which an increase in the carbon to nutrient ratio in

phytoplankton, triggered by an increase in light, induces a decrease in zooplankton (carbon) assimilation efficiency, concluding that an increase in energy (light) is not of advantage to the whole system but only for the primary producers (i.e. the paradox of energy enrichment).

Although these mechanisms are experimentally well documented and various theoretical and mechanistic models have been developed on them (Loladze et al., 2004; Hall et al., 2004; Mitra, 2006; Diehl, 2007; Stief et al., 2010; Elser et al., 2012), they have never been tested in relation to the phytoplankton bloom formation under realistic seasonally changing environmental conditions (i.e., nutrient and light). Furthermore, the effect of phytoplankton nutritional quality on grazers has never been implemented in a fully structured marine ecosystem model. Typically, marine ecosystem models are poor at describing zooplankton grazing as they often have very rigid food webs (Sailley et al., 2013; Mitra et al., 2014) and this strongly limits their utilization for the investigation of predator-prey dynamics.

The effect of phytoplankton quality (described as nutrient stoichiometry) on the ingestion and assimilation efficiencies of a consumer has been termed **S**toichiometric **M**odulation of **P**redation (SMP, Mitra 2006). The importance of inclusion of SMP when simulating planktonic predator-prey interactions against experimental datasets has been demonstrated for both micro- and meso-zooplankton (Mitra, 2006; Mitra and Flynn 2006; Mitra and Flynn 2007). Mitra (2006) in particular has shown that the inclusion of SMP in a zooplankton model significantly improved the simulation of the interactions between the microzooplankton *Oxyrrhis marina* and the phytoplankton *Isochrysis galbana* observed by Flynn and Davidson (1993). However, these studies have mainly focussed on model validation using laboratory data; i.e., SMP has not been tested in a realistic ecosystem framework.

In this paper, we have integrated the SMP (Mitra, 2006) into the European Regional Seas Ecosystem Model (ERSEM, Blackford et al., 2004) with the aim to explore how the combination of abiotic factors (e.g., NHF) and biotic mechanisms (e.g., SMP) impact on plankton bloom dynamics. To this end, the revised version of ERSEM (hereafter ERSEM-SMP) has been coupled with the General Ocean Turbulence Model (GOTM, Burchard et al 1999), implemented at the station L4 (50° 15'N, 4° 13'W) and tested against the high frequency observations at that site. Our working hypothesis is that the increase in light exposure experienced by diatoms in the transition between winter and spring may result in changes in the internal stoichiometry of the diatoms, reducing grazing pressure and thence favouring increase in their biomass.

We focus on station L4 because it has an extensive time series data of phytoplankton and zooplankton abundance, coupled with measurements of physical properties and nutrients. In addition to diatoms, the dominant primary producers, *Phaeocystis* blooms are also regularly observed at this site with intense but short-lived peaks during spring. Coccolithophorids may also occasionally bloom but rarely attain the high cellular density of diatoms (Widdicombe et al., 2010). Microzooplankton are observed to peak concomitantly (typically ciliates) or just after (heterotrophic dinoflagellates) the diatom bloom, albeit with high variability in timings from year to year (Atkinson et al. this issue). This group achieves a higher biomass at L4 than mesozooplankton (Atkinson et al. this issue) and due to higher specific metabolic rates is likely to dominate the grazing impact (Calbet and Landry, 2004; Irigoien et al., 2005; Bautista and Harris, 1992; Atkinson et al., unpublished data). Simulation of phytoplankton internal stoichiometry and biomass, along with microzooplankton biomass, grazing and assimilation efficiency were critically analysed and used to test our hypothesis. Simulated diatoms, microzooplankton and nutrients were compared with available in situ data.

THE MODEL

ERSEM is a bulk biomass functional group ecosystem model describing the nutrient and carbon cycle within the lower trophic levels of the marine ecosystem. Model state variables include living organisms, dissolved nutrients, organic detritus, oxygen and CO_2. A key feature of ERSEM is the decoupling between carbon and nutrient dynamics allowing the simulation of variable stoichiometry within the modelled organisms. Chlorophyll is also treated as an independent state variable following the formulation proposed by Geider et al. (1996). Consequently, each plankton group is modelled using up to five state variables describing each cellular component: carbon, nitrogen, phosphorus, silicon (only for diatoms) and chlorophyll-a. These features make ERSEM particularly suitable for this work.

In order to test our hypothesis which specifically focuses on the diatoms-microzooplankton grazing interactions, we have simplified the standard ERSEM food web described in Blackford et al (2004) as shown in Fig. 1. The rationale behind this is to "isolate", as far as possible, the biotic processes to be investigated (e.g., diatom quality and allied impact on microzooplankton growth dynamics) and therefore making it easier to quantify their relevance. Thus, our model is based on a predator-prey system (accounting for SMP) comprising of diatoms (P1), considered as the dominant bloom-forming phytoplankton at L4 and microzooplankton (Z1) considered as the dominant grazers of diatoms; Z1 represents the fraction of microzooplankton (e.g., dinoflagellates such as *Gyrodinium* and *Protoperidinium*; ~ ESD > 20 μm) large enough to graze diatoms. To make the system more realistic and consistent with the L4 observations, we have also introduced a second phytoplankton functional group accounting for small (non-diatoms) phytoplankton (P2) and their grazers (Z2). P2 includes a variety of groups (e.g., nanoflagellates and *Phaeocystis*) expressing a wide range of traits and thus represents generic autotrophic activity at a lower size range; i.e.,

P2 has been included to ensure that diatoms have competitors for nutrients at the beginning of the bloom. Z2 represents the smaller fraction of microzooplankton (i.e., ciliates such as *Strombidium*) assumed to be specialised to feed on phytoplankton (mainly nanoflagellates) smaller than blooming diatoms.

Finally, a top closure mimicking the mesozooplankton grazing on microzooplankton is represented by Z3. The interactions between P2 and Z2, and Z3 and Z1 are modelled through the standard ERSEM formulation (Blackford et al., 2004) without the inclusion of SMP. Z2 and Z3 do not have predators within the model but they are assumed to cannibalize (Fig 1) and thus mimicking a density dependent top down closure. Bacteria are not explicitly modelled but are implicitly represented through remineralisation of detritus (equal to 0.05 d^{-1}) producing dissolved nutrients and CO_2.

As we focus on the formation and evolution of diatom blooms occurring between April and July we did not consider the autotrophic dinoflagellates, which usually bloom in late summer and/or early autumn (Widdicombe et al., 2010). It is worthwhile to recall that this simplified food web is not meant to represent the entire plankton community with allied complexities in their interactions as observed at L4, rather our aim is to focus on one specific process.

Silica regeneration in the water column is not considered in the standard ERSEM formulation where biogenic silica is assumed to be regenerated only via the benthic compartment. However, in order to prevent extreme silica limitation we have assumed a simple first order silica remineralisation converting biogenic particulate silica to dissolved silica at a fixed rate of 0.1 d^{-1}. This simple assumption is consistent with experimental evidences suggesting that up to 50% of the biogenic silica (opal) is re-generated in the euphotic zone (Sarmiento and Gruber, 2006).

A complete description of the equations, basic assumptions and underlying philosophy of ERSEM can be found in Blackford et al. (2004). Here we limit our description to the formulation describing Z1 which is the only part of the model altered with respect to the original model. The general equation for Z1 carbon biomass is given by the balance between grazing (gra), and loss terms due to respiration (res), excretion (exc), natural (non-predation) mortality ($mort$) and predation mortality ($pred$):

$$\frac{dZ}{dt} = \left.\frac{dZ}{dt}\right|^{gra} - \left.\frac{dZ}{dt}\right|^{res} - \left.\frac{dZ}{dt}\right|^{exc} - \left.\frac{dZ}{dt}\right|^{mort} - \left.\frac{dZ}{dt}\right|^{pred} \quad (1)$$

Grazing is described using a "potential" grazing term ($grazing'$) multiplied by a factor taking into account the nutritional quality of the prey:

$$\left.\frac{dZ}{dt}\right|^{gra} = grazing' * FQ \quad (2)$$

FQ is the function linking the potential grazing to the stoichiometry of phytoplankton described below (equation 6). $grazing'$ is described using the classical Michaelis-Menten formulation as reported in Blackford et al., (2004):

$$grazing' = Z * temp * r\frac{P\prime}{P\prime + K} \quad (3)$$

Where Z is the zooplankton biomass, $temp$ is a function accounting for the temperature dependency, r the potential grazing rate and P' the available food. K is the half saturation constant for food. P' is given by the biomass of the prey (P) multiplied by a parameter representing the "preference" for that particular prey (P_f) and scaled by a Michaelis Menten

function accounting for a food threshold parameter ($minfood$) which prevents excessive grazing of scarce prey:

$$P' = P_f * P * \frac{P}{P+minfood} \quad (4)$$

The function $temp$ describes an enhancement of physiological processes with the increase of temperature following a Q_{10} function:

$$temp = Q_{10}^{\left(\frac{(T-10)}{10}\right)} \quad (5)$$

FQ is a function linking the grazing with the nutritional quality of the phytoplankton, described here using nutrient stoichiometry and is given by:

$$FQ = 1 + \left[1 - min\left(\frac{qpP}{qpZ}, \frac{qnP}{qnZ}, 1\right)\right] * a \quad (6)$$

where qpP and qpZ are the phosphorus to carbon (P:C) ratios of phytoplankton and zooplankton respectively, and qnP and qnZ are the nitrogen to carbon (N:C) ratios in phytoplankton and zooplankton respectively. a is the parameter describing the response of the grazers to the decrease in quality of the prey (Mitra, 2006). In this work we have assumed a decrease of ingestion associated with low nutrient content of the prey (i.e., decrease in palatability) and as such, we have considered a equal to -1.

Respiration is composed of a basal component (depending on biomass) and a metabolic-activity related component (depending on ingestion):

$$\left.\frac{dZ}{dt}\right|^{res} = R_r * temp * Z + \left.\frac{dZ}{dt}\right|^{gra} * A_r * AE \quad (7)$$

Assimilation efficiency (AE) is assumed to vary between a minimum and a maximum value (assumed to be 0.25 and 0.75, respectively) and is given by:

$$AE = AE_{min} + (AE_{max} - AE_{min}) * FQ_{AE} \quad (8)$$

where FQ_{AE} is the function linking the phytoplankton quality (C:N:P) to the assimilation efficiency of zooplankton (Mitra, 2006) and is given by:

$$FQ_{AE} = \min(1, N_{lim}, P_{lim}) * (1 + K_{AE}) min\left(1, \frac{qpP}{qpZ}, \frac{qnP}{qnZ}\right) \quad (9)$$

In Eq. 9, K_{AE} is the half saturation constant as described in Mitra (2006)

N_{lim} and P_{lim} are two Michaelis Menten-like functions given by:

$$N_{lim} = \frac{\frac{qnP}{qn_{max}}}{\frac{qnP}{qn_{max}} + K_{AE}} \quad (9.1)$$

and

$$P_{lim} = \frac{\frac{qpP}{qp_{max}}}{\frac{qpP}{qp_{max}} + K_{AE}} \quad (9.2)$$

qp_{max} and qn_{max} are the maximum phytoplankton P and N quota (i.e., N:C and P:C ratios), respectively, assumed to be equal to the double of the nutrient content implied by the Redfield ratio (Blackford et al., 2004, Table 3)

Loss term due to excretion is governed by the following equation:

$$\left.\frac{dZ}{dt}\right|^{exc} = \left.\frac{dZ}{dt}\right|^{gra} * (1 - AE) \quad (10)$$

Non-predation mortality loss is assumed to be composed by a constant term plus an additional fraction triggered by low oxygen concentration

$$\left.\frac{dZ}{dt}\right|^{mort} = Z * \left((1 - eO_2) * r_{mortox} + r_{mort}\right) \quad (11)$$

r_{mort} and r_{mortox} are the background mortality rate and the mortality rate at low oxygen concentration, respectively. eO_2 is an oxygen limitation factor calculated from the relative oxygen saturation (O_{rel}) and the half saturation mortality rate constant (h_{oxmort}):

$$eO_2 = (1 + h_{oxmort}) * \left(\frac{O_{rel}}{O_{rel}+h_{oxmort}}\right) \quad (12)$$

The ingestion of nutrient via grazing is derived by equation 3 and reflects the nutrient content of the ingested prey. In the same way, the loss of nutrient via excretion, mortality and predation is depending on the carbon to nutrient ratio of zooplankton. Additionally, any nutrient in excess of a threshold value ($qZ_{max}^{N.P}$) is assumed to be directly excreted to the inorganic pool (phosphate and ammonium).

Model parameters describing the communities Z1, Z2 and Z3 are listed in Table 1. The parameters for the phytoplankton functional groups P1 and P2 are the same as in Blackford et al., (2004). However, a few changes were required to improve our simulation at L4: i) the potential photosynthetic rate of P2 was lowered from 2.7 to 2.0 d^{-1}; ii) different maximum chlorophyll to carbon ratios were employed for the two phytoplankton groups (0.04 for P1 and 0.03 for P2; consistent with literature values (Geider et al. 1997)), and iii) the reference silica to carbon ratio for diatoms has been lowered to 0.01 (mmol S (mg C)$^{-1}$) as reported in Vichi et al. (2006).

PHYSICAL SETUP AND OBSERVATIONAL DATA

The GOTM-ERSEM set up used in this work is identical to that described in Polimene et al., (2014). The model is forced with reanalysis meteorological data (ECMWF) and initialised with temperature, salinity and nutrient concentrations observed *in situ* (Smyth et al., 2010). At the lower boundary of the water column a simple remineralisation closure is applied exporting sinking detritus that is re-injected into the water column as dissolved nutrients and inorganic carbon at a fixed rate of 0.05 d^{-1}.

Surface radiation is calculated by an astronomical formula (Rosati and Miyacoda, 1988) taking into account latitude, longitude, time, fractional cloud cover and albedo. Light extinction through the water column is assumed to be dependent on water mass, i.e. organic particulates in the water column (both living and detritus) and silt, as described in Blackford et al (2004). The total surface heat flux Q_{tot} is calculated as the sum of the latent heat flux Q_E, the sensible heat flux Q_H, and the long wave back radiation Q_b. Each of these fluxes are calculated by using the bulk formulae of Kondo (1975). The net heat flux (NHF) is then calculated by summing the incident short wave radiation to the total heat fluxes. The model was run for 10 years (2000-2009) after 4 years of spin up.

The observational data used in this work (Woodward et al., 2013; Widdicombe et al 2010) were obtained under the weekly sampling strategy of the Western Channel Observatory (WCO, http://www.westernchannelobservatory.org.uk/). The description of the methodology used for samples collection and cell enumeration of phytoplankton and microzooplankton can be found in Widdicombe et al., (2010). Cell volumes are calculated according to the equations of Kovala and Larrance (1996) and converted to carbon using the equations of Menden-Deuer and Lessard (2000).

SENSITIVITY ANALYSIS

A quantitative sensitivity analysis (SA) was carried out to investigate the changes introduced by the SMP formulation to the ERSEM simulations. We applied a Monte-Carlo based approach (see, e.g., Saltelli et al, 2005, Pastres and Ciavatta, 2005) to rank the sensitivities of a target model output y (the annual average of the grazing efficiency) with respect to the model parameters that were handled in this work (i.e., the parameters in Table 1 and the phytoplankton parameters altered with respect to Blackford et al., (2004)). The SA included also the initial conditions of nitrate and phosphate. The *m* model parameters and nutrient initial conditions defined the "input factor" vector (Table 2) of the SA, $\mathbf{X_i} = (X_1,.., X_j, \ldots,X_m)$. A number (i=1,2,…,) of n random realizations of the vector were obtained by sampling uniform probability distributions defined for the input factors (Table 2). Each realization is used to run a model simulation that provides a scalar output y_i.

The input-output relationship was represented by means of a multiple linear regression model $\mathbf{y} = \mathbf{X}\ \mathbf{b} + \cdot\boldsymbol{\varepsilon}$, and the *m* absolute values of the standardized regression coefficients β_j are the sensitivity indices that provides the rank of the input factors (e.g. Saltelli et al., 2000; Pastres and Ciavatta, 2005). The SA was carried out, for both ERSEM and ERSEM SMP, by running n=1000 model simulations of the year 2000, after a four year spin-up. The same probability density functions of the input factors were applied in the two model configurations to make the rankings inter-comparable. The rankings of the parameters for the two models (ERSEM and ERSEM-SMP) were compared to discuss the importance of the SMP "mechanism" with respect to the tuning of the model parameters in simulating the target variable.

We note that the regression coefficients provide meaningful rankings only when the linear model explains relatively large fractions of the model output variability (Saltelli et al., 2000). In our application we verified that the determination coefficients (R^2) of the linear models

were higher than 70% and statistically significant (F-statistic for linear versus constant model; $p<0.001$).

RESULTS

Simulated and observed, monthly averaged, diatoms and microzooplankton biomass, nitrate phosphate and silicate are displayed in Fig 2. The qualitative agreement between model and observations is evaluated through the Spearman's correlation index between simulated and observed variables shown in Table 3. The correlation coefficient is higher than 0.6 for microzooplankton and nutrients and equal to 0.35 for diatoms. The correlation indices concerning the simulations carried out with the standard ERSEM model are also reported for comparison.

The seasonal evolution of simulated air-sea net heat flux (NHF), surface turbulent kinetic energy (TKE) and mixed layer depth (MLD) is depicted in Fig 3. NHF is negative from January to March, switching to positive in April. After the summer, NHF reverts back to negative in September. The transition between winter and spring (March-April) is also characterized by a reduction in TKE (from 0.0007 to < 0.0004 m^{-2} s^{-2}).TKE increases after the summer, returning to values comparable with those simulated in winter. The simulated seasonal cycle of the MLD implies that in April and May phytoplankton are exposed more to light due to being "confined" in the first 10-15 metres of the water column. Simulated average irradiance within the mixed layer depth is 24 W m^{-2} in March and 115 W m^{-2} in April. These results are consistent with the description of the physical conditions underpinning the onset of phytoplankton bloom reported in Smyth et al. (2014).

Figure 4 shows that the diatom carbon to phosphorus and carbon to nitrogen ratios are low in winter, they start to increase in spring (corresponding with the bloom) reaching the maximum level in summer. It is worth noting that the carbon to nutrient ratios simulated in all our experiments are comparable with the values reported in literature for marine particulate organic matter (Geider and La Roche, 2002). Microzooplankton assimilation efficiency follows the opposite trend being high in winter, decreasing in spring (in correspondence of the sharp increase of diatoms biomass) and reaching the lowest level in summer. The grazing flux, in contrast, reaches the maximum level in May, corresponding to the highest diatom biomass.

Higher phytoplankton biomass (Fig. 5) does not correspond to higher nutrient content which, in contrast, coincides with the higher zooplankton assimilation efficiency. Notably, the grazing flux, when taken on a daily basis, is less tightly related to the prey biomass. Higher grazing rates, correspond to intermediate levels of biomass (between 50 and 150 mg C m^{-3}) and an intermediate level of the prey nutrient quota (C:P ~80-95 and C:N ~4-5.5). Diatoms, at the peak of the bloom (Fig. 6), are characterized by a decrease in the nutrient to carbon ratios with respect to pre bloom conditions. The declining part of the bloom is characterized by a slow increase in cellular nutrient content due to the release of carbon via exudation (Fig. 6) which enhances grazing activity. As a result, the grazing flux and the microzooplankton biomass reach the highest value at the end of the bloom.

The sensitivity of the ERSEM-SMP model to decrease in the concentrations of phosphate and nitrate, given as model initial conditions (50% reduction was investigated) is shown in Fig. 7 and Fig. 8. Lowering nutrient concentrations causes diatoms to become more nutritionally imbalanced and therefore, less palatable to zooplankton. This leads to a counterintuitive response that fewer nutrients produce a higher peak (in term of carbon) during the bloom (Fig. 7). A simulation carried out by decreasing nitrate and phosphate initial conditions by

352 25% (data not shown) showed the same qualitative (but less intense) response, with a slight
353 increase in diatom carbon biomass and a concomitant decrease in zooplankton biomass. Only
354 when the initial nitrate and phosphate conditions are decreased by 75% (data not shown) do
355 we see a clear decrease in diatom biomass. Model simulations performed with the standard
356 ERSEM formulation (i.e. without SMP, and a fixed assimilation efficiency of 50%) applied
357 to the same model foodweb (Fig 1) are shown in Fig 9. In this case diatoms never manage to
358 bloom and the system is dominated by microzooplankton. By decreasing the initial
359 concentration of nitrate and phosphate by 50%, the system does not show substantial changes
360 in behaviour (Fig. 10).

361 A Monte Carlo based sensitivity analysis on both ERSEM-SMP and ERSEM has been
362 performed in order to assess to what extent the above described results are affected by the
363 choice of selected parameters and nutrient initial conditions (Table 2). As the essence of the
364 SMP is the effect of the phytoplankton nutritional status on the grazing activity, we have
365 selected as target variable of our analysis the grazing efficiency of the model
366 microzooplankton Z1. The results of this analysis are presented in Table 4 where each input
367 factor (Table 2) is ranked on the base of its capacity to affect the simulation of the target
368 variable. In both the models, the parameters defining the half saturation constant for food and
369 prey "preference" (K(Z1) and Pf(P1-Z1), respectively) are the most important. However,
370 Table 4 highlights that with the addition of the SMP, the initial condition of the limiting
371 nutrient is considerably more important for the simulation of the grazing activity of Z1 over
372 P1. PO_4 in table 4 ranked 6th and 18th for ERSEM-SMP and ERSEM, respectively.
373 Furthermore, the ERSEM-SMP simulations of grazing efficiency have relatively low
374 sensitivity with respect to the values of the SMP-parameters. Indeed, the new parameters
375 introduced for the implementation of the SMP (AE_{max}, AE_{min}, and K_{AE}) ranked relatively low
376 (9, 17 and 24, respectively). This suggests that the ERSEM-SMP simulations depend more on

the process/mechanism described in the model than on the numerical values of the parameters.

An additional sensitivity analysis has been performed by manually altering some key zooplankton parameters and nutrient initial condition (Table 5) in the ERSEM model (Fig. 11). The rationale behind this experiment was to further investigate whether, by tuning specific parameters, the standard ERSEM can produce simulations comparable to the ones of ERSEM-SMP.

Figure 11 shows that by changing the half saturation constant for food (K) and the food threshold ($minfood$), the simulation does not display significant changes: the system is, in all the three experiments, dominated by microzooplankton. Only by assuming a greater predatory pressure on microzooplankton (by increasing the value of the parameter P_f, experiment S5) do diatoms manage to bloom exceeding zooplankton biomass. The sensitivity experiment S5 is the model setup under which ERSEM produces the closest simulation to ERSEM-SMP. However, even under these conditions, by reducing the initial nutrient conditions by 50% the standard ERSEM does not display the behaviour simulated by the SMP-ERSEM model, further confirming the results displayed in Table 4.

DISCUSSION

Our simulations suggest that the increase in light exposure experienced by diatoms between March and April decouples photosynthesis from nutrient uptake, thereby altering cellular stoichiometry. The increase in the cellular carbon to nutrient ratio of the diatoms decreases their palatability thence reducing both grazing and assimilation efficiency of the microzooplankton. We suggest that these changes contribute to the formation of the diatom

bloom regularly observed at the station L4. A conceptual model describing the formation and evolution of a diatom bloom is depicted in Fig. 12.

During winter, diatoms are limited by the amount of light but are also controlled through grazing pressure exerted by large microzooplankton (modelled through the variable Z1). During this time of the year, high environmental nutrient concentrations allow diatoms to be rich in nutrients (such as N and P) and, consequently, zooplankton assimilation efficiency is also high. Changes in physical conditions, such as reduced turbulence and increased surface water temperature (Smyth et al., 2014 and Fig 3), increases the phytoplankton residence time in the well-lit zone of the water column (Fig 3) and desynchronize photosynthesis from nutrient uptake. This increases the amount of cellular carbon with respect to nutrients. Less nutrient content, decreasing diatom palatability, reduces the activity of microzooplankton, allowing diatoms to "escape" from being top down controlled and thus to bloom.

Bloom conditions for diatoms are therefore a compromise between attaining high nutrient cellular content (i.e., high food quality), where the diatom population are controlled by zooplankton grazing, and poor nutrient cellular content under which diatoms (although "escaping" zooplankton grazing) are too nutrient stressed for growth. The former condition takes place in winter, the latter in summer. The conditions leading to the bloom occur in the spring period when the nutrient condition of diatoms are at an intermediate level which still allows a positive growth but, at the same time, a reduced palatability.

The idea that reduced cell nutrient content be advantageous for primary producers has been previously used in evolutionary modelling work (Branco et al., 2010). The generic model proposed by these authors implied that phytoplankton with intermediate nutrient uptake rates are less palatable for herbivores. In this way, some phytoplankton species gain a competitive advantage over competitors that have higher affinity for nutrients and are therefore more

susceptible to grazers. Here, we have shown that the same concept can be important within a single phytoplankton group on a seasonal scale.

Including SMP makes the modelled predator-prey interactions sensitive to the availability of nitrate and phosphate. As expected, the simulations with low nutrient concentrations show that diatoms are more stoichiometrically imbalanced and therefore less palatable for zooplankton when the availability of nitrate and phosphate is low. Consequently, diatoms produce a higher peak (in terms of carbon) during the bloom (Fig. 5). This suggests that decreasing the food quality (more than the quantity) of primary producers, reduces the transfer of carbon from the algal producers to the higher trophic levels of the food chain. This may have profound effects on the ecosystem responses to climate change, particularly in regions where the surface waters are expected to become more oligotrophic (Polovina et al., 2008). Sensitivity experiments showed in Table 4 and Fig. 11 show that the standard ERSEM grazing parameterisation does not reproduce this kind of dynamics. More in general, the sensitivity analysis highlights that the SMP as “mechanism” is more relevant in impacting the model simulation of the grazing efficiency then the numerical values of the parameters used. This strengthens the case for exploring the inclusion of SMP in marine ecosystem models used for climate change simulations.

Particular attention should be paid to the role of silica in the aforementioned mechanism. Silica is not required for zooplankton growth and therefore is not included in the SMP formulation implemented here. Furthermore, silica is assumed to limit directly primary production in ERSEM (Ebenhoh et al., 1997; Blackford et al., 2004) with the consequence that silica is coupled more with carbon than nitrogen or phosphorous. Reduced availability of silica also implies a reduced fixation of carbon and therefore a more balanced carbon to nitrogen and phosphorus cellular ratio. Consequently, the above described dynamics is not simulated when silica is the limiting nutrient.

The importance of food quality as a consequence of skewed nutrient stoichiometry which in turn is induced by an "imbalance" in the supply of nutrients and light has previously been stressed in laboratory experiments (Urabe and Sterner, 1996; Hessen et al., 2002) and theoretical modelling studies (Loladze et al., 2000; Loladze et al., 2004; Hall et al., 2004; Mitra, 2006; Diehl, 2007; Elser et al., 2012). We have related phytoplankton palatability to the physical environment (Fig. 3) and have proposed a conceptual model (Fig. 12), describing bloom formation and evolution, which connects physical constrains (heat flux, turbulence, mixed layer depth) physiological status of phytoplankton (i.e., cellular stoichiometry) and grazing. These connections are summarised in Fig. 13 which shows the correlation between heat fluxes and cellular stoichiometry($r=0.88$, $p<0.001$), an emergent property of our model. While confirming that the switch of NHF from negative to positive described by Smyth et al. (2014) is a prerequisite for the bloom formation, our model also suggests that, after the onset of the proper physical conditions, phytoplankton decrease in palatability and reduced zooplankton grazing pressure play a significant role in the formation of a bloom.

We have shown that a combination of abiotic and biotic factors work synergistically to impact on the plankton bloom dynamics. The behaviour shown by the present model is consistent with the "paradox of energy enrichment" hypothesised by Loladze et al. (2000): when more energy is supplied to the system (steep increase in light) a decoupling between carbon and nutrient is induced. The latter decreases the "quality" of the prey which, being less suitable for the predator, reaches its highest concentration. Our model also supports the general concept of the "loophole" hypothesis (Irigoien et al., 2005; Kiørboe, 2008). These authors, investigating the biological dynamics underpinning a phytoplankton bloom invoked a set of mechanisms including physical (e.g., size, colony-formation, spines, frustules and coccoliths) and chemical (e.g., DMSP production) defence leading to a decrease of palatability of phytoplankton and to a decrease (loophole) of the grazing pressure. Our

simulations and the consequent conceptual model depicted in Fig.12 suggest that the decrease of the phytoplankton nutrient to carbon ratio (and the subsequent decrease in phytoplankton palatability) could play a pivotal role in creating the "loophole" through which diatoms manage to bloom.

Although these results support our hypothesis, we recognise that only with specific, purposely performed, field measurements will we be able to properly assess the mechanism described in Fig. 12. In particular, we require data on the temporal evolution of the phytoplankton cellular nitrogen and phosphorus with respect to carbon content; these are currently lacking. Also, time series measurements of micro- and meso-zooplankton grazing, looking both at mass specific ingestion rates and total grazing pressure, would shed light on the complex dynamics surrounding the start of a bloom. One of the advantages of modelling work like this is to highlight gaps and inconsistencies in current knowledge and datasets, and thence to inform and drive future experimental research.

ACKNOWLEDGMENTS

The authors would like to thank the PML crew of RV Quest and the PML staff involved in the sampling of the Plymouth L4 site. Nutrient data used in Fig 2 were analysed by Carolyn Harris and Malcolm Woodward.

LP was part funded by the EC FP7 My Ocean project. AA and LP were part funded through the UK NERC-Defra Shelf Seas Biogeochemistry program. JIA and AM were part funded thought the EC FP7 Euro Basin project. AM was part funded by the NERC UK project

iMarNet NE/K001345/1. SC was part funded by the NERC National Centre of Earth Observation (NCEO). AA, CW, JIA, LP, SS and SC were part funded through NERC National Capability, in sustained observations and marine modelling.

Table 1. Zooplankton parameters

Prameter	Notation	Unit	Z1	Z2	Z3	Reference
Q_{10} value	Q_{10}	adim	2	2	2	Blackford et al (2004)
Grazing rate at 10 C	r	d^{-1}	1.2	2.0	0.5	Blackford et al (2004)
Half saturation constant for food	K	mg C m^{-3}	10	10	40	This study/ Blackford et al (2004)
Food threshold	$minfood$	mg C m^{-3}	2.5	10	1.0	This study/ Blackford et al (2004)
Fraction of food respired	A_r	d^{-1}	0.5	0.4	0.6	This study/ Blackford et al (2004)
Constant Assimilation efficiency (Z2 and Z3)	AE	adim	N/A	0.5	0.5	Blackford et al (2004)
Min Assimilation efficiency	AE_{min}	adim	0.25	N/A	N/A	This study
Max Assimilation efficiency	AE_{max}	adim	0.75	N/A	N/A	This study
Half saturation constant for AE	K_{AE}	adim	1			Mitra (2006)
Rest respiration rate	R_r	d^{-1}	0.02	0.02	0.02	Blackford et al (2004)
Mortality rate	r_{mort}	d^{-1}	0.05	0.05	0.05	Blackford et al (2004)
Mortality rate due to low oxygen	r_{mortox}	d^{-1}	0.25	0.25	0.25	Blackford et al (2004)
Michaelis Menten constant for oxygen limitation	h_{oxmort}	mmol m^{-3}	7.8125	7.8125	7.8125	Blackford et al (2004)
Max N:C	qZ^N_{max}	mmol N (mg C)$^{-1}$	0.0167	0.0167	N/A*	Blackford et al (2004)
Max P:C	qZ^P_{max}	mmol P (mg C)$^{-1}$	0.001	0.001	N/A*	Blackford et al (2004)
Available fraction of prey (P1 for Z1, P2 for Z2 and Z1 for Z3)	P_f	adim	1	1	0.5	This study

*Mesozooplankton are assumed to have a fixed internal stoichiometry (Blackford et al., 2004)

Table 2 Input factors of the Monte Carlo based sensitivity analysis, their nominal values and the range minimum-maximum of their uniform probability distributions. The notations of the parameters are specified in Table 1 (but see notes c and d)

Notation	Nominal	minimum	Maximum	Notes
K(Z1)	10	1	60	
Pf(P1-Z1)	1	0.1	1	
Chl:Cmax(P1)	0.04	0.01	0.07	c
K(Z3)	40	1	60	
Pf(P2-Z2)	1	0.1	1	
PO_4	0.4	0.2	0.6	d
r(Z1)	0.02	0.014	0.026	*
K(Z2)	10	1	60	
AEmax(Z1)	0.25	0.1	0.499	a
qZPmax(Z1)	0.0167	0.01169	0.02171	*
Ar(Z1)	0.5	0.35	0.65	*
rmort(Z1)	0.25	0.175	0.325	*
minfood(Z1)	2.5	1	20	
Pf(Z1-Z3)	0.5	0.1	1	
qsP1c	0.01	0.01	0.03	c
NO_3	8	4	12	d
AEmin(Z1)	2	1.4	2.6	*a
r(Z2)	1.2	0.84	1.56	*
Q10(Z1)	0.4	0.28	0.52	*
Rr(Z1)	0.05	0.035	0.065	*
Ar(Z2)	0.5	0.35	0.65	*
Q10(Z2)	2	1.4	2.6	*
r(Z3)	0.5	0.35	0.65	*
KAE(Z1)	0.75	0.5	0.9	a
minfood(Z3)	1	0.1	10	
qZPmax(Z2)	0.0012	0.00084	0.00156	*
qZNmax(Z1)	2	1.4	2.6	*
Chl:Cmax(P2)	0.03	0.01	0.07	c
r(P2)	2	1.5	3	c
rmortox(Z3)	0.25	0.175	0.325	*
rmort(Z3)	0.05	0.035	0.065	*
AE(Z3)	0.5	0.1	0.9	
hoxmort(Z3)	7.8125	5.46875	10.15625	*
hoxmort(Z1)	7.8125	5.46875	10.15625	*
Rr(Z2)	0.02	0.014	0.026	*
Rr(Z3)	0.02	0.014	0.026	*
minfood(Z2)	10	1	20	
rmort(Z2)	0.25	0.175	0.325	*
AE(Z2)	0.5	0.1	0.9	
rmortox(Z1)	0.001	0.0007	0.0013	*
qZNmax(Z2)	0.0167	0.01169	0.02171	*
Q_{10}(Z3)	2	1.4	2.6	*
hoxmort(Z2)	7.8125	5.46875	10.15625	*
rmortox(Z2)	0.05	0.035	0.065	*
AE(Z5)	0.5	0.1	0.9	b

Notes. * : the range minimum-maximum is defined as the nominal value ±30% of the value itself; a) parameters included in ERSEM SMP only; b) parameters included in ERSEM only; c) phytoplankton parameters for P1 and P2 not defined in Table 1 (Chl:Cmax = maximum chlorophyll-to-carbon ratio [mgChl $(mgC)^{-1}$]; r = potential photosynthetic rate [d^{-1}]; qsP1c = maximum silica to carbon ratio in diatoms [mmolSi $(mgC)^{-1}$]); d) initial conditions of nutrients (PO4 = phosphate [mmol m^{-3}]; NO3 = nitrate [mmol m^{-3}]).

Table 3. Spearman rank correlation between modelled and observed variables ($p<0.001$)

	diatoms	**microzoo**	**PO_4**	**NO_3**	**Si**
ERSEM-SMP	0.35	0.80	0.61	0.80	0.67
ERSEM	-0.16*	0.82	0.65	0.81	0.65

*p=0.07

Table 4. Results of the Monte Carlo sensitivity analysis of ERSEM SMP (left) and ERSEM (right). Ranking of the input factors (i.e. model parameters and initial conditions of nitrate and phosphate) based on computed standardized linear regression coefficients β. N.S. indicates parameters having β values that were not significantly different from zero (t-statistic; $p < 0.05$).

ERSEM SMP	Rank	ERSEM	Rank
K(Z1)	1	K(Z1)	1
Pf(P1-Z1)	2	Pf(P1-Z1)	2
Chl:Cmax(P1)	3	K(Z3)	3
K(Z3)	4	Pf(P2-Z2)	4
Pf(P2-Z2)	5	K(Z2)	5
PO_4	6	Chl:Cmax(P1)	6
r(Z1)	7	minfood(Z1)	7
K(Z2)	8	Pf(Z1-Z3)	8
AEmax(Z1)	9	r(Z1)	9
qZPmax(Z1)	10	qsP1c	10
Ar(Z1)	11	Ar(Z1)	11
rmort(Z1)	12	r(Z3)	12
minfood(Z1)	13	minfood(Z2)	13
Pf(Z1-Z3)	14	r(Z2)	14
qsP1c	15	r(P2)	15
NO_3	16	Ar(Z2)	16
AEmin(Z1)	17	minfood(Z3)	17
r(Z2)	18	PO_4	18
Q10(Z1)	19	NO_3	19
Rr(Z1)	20	AE(Z3)	20
Ar(Z2)	21	rmort(Z1)	21
Q10(Z2)	22	Chl:Cmax(P2)	22
r(Z3)	23	Q10(Z1)	23
KAE(Z1)	24	rmort(Z3)	24
minfood(Z3)	25	Rr(Z1)	25
qZPmax(Z2)	26	Q10(Z2)	26
qZNmax(Z1)	27	rmortox(Z3)	N.S
Chl:Cmax(P2)	28	Rr(Z2)	N.S
r(P2)	29	Q_{10}(Z3)	N.S
rmortox(Z3)	N.S	qZPmax(Z1)	N.S
rmort(Z3)	N.S	hoxmort(Z3)	N.S
AE(Z3)	N.S	rmort(Z2)	N.S
hoxmort(Z3)	N.S	hoxmort(Z1)	N.S
hoxmort(Z1)	N.S	AE(Z2)	N.S
Rr(Z2)	N.S	Rr(Z3)	N.S
Rr(Z3)	N.S	qZPmax(Z2)	N.S
minfood(Z2)	N.S	qZNmax(Z2)	N.S
rmort(Z2)	N.S	rmortox(Z2)	N.S
AE(Z2)	N.S	qZNmax(Z1)	N.S
rmortox(Z1)	N.S	hoxmort(Z2)	N.S
qZNmax(Z2)	N.S	AE(Z1)	N.S
Q_{10}(Z3)	N.S	rmortox(Z1)	N.S
hoxmort(Z2)	N.S		
rmortox(Z2)	N.S		

Table 5. Sensitivity experiments on key zooplankton parameters for the standard ERSEM model

experiment	**Parameters**		
	K	$minfood$	P_f (Z1 for Z3)
S1	45	2.5	0.5
S2	60	2.5	0.5
S3	60	10	0.5
S4	60	10	0.8
S5	60	10	1.0
S6	As S5 but with reduced (50%) initial nutrient (N and P) conditions		

FIGURE CAPTIONS

Fig 1. Schematic of the modelled food interactions. Dotted arrows indicate density-dependent mortality closure, for example cannibalism

Fig 2. Modelled and observed time series of (A) diatom biomass; (B) microzooplankton biomass; (C) phosphate; (D) nitrate; (E) silicate. Both observations and simulations are monthly averages for the period 2000-2009. Units are mg C m^{-3} for biomasses and mmol m^{-3} for nutrients. Modelled microzooplankton is the sum of Z1 and Z2.

Fig 3. Climatological, monthly averaged, simulated (A) Net Heat Flux (NHF, W m^{-2}); (B) surface Turbulent Kinetic Energy (TKE, m^{-2} s^{-2}) and (C) Mixed Layer Depth (MLD, metres)

Fig 4. Climatological, monthly averaged, simulated diatom (P1) and microzooplankton (Z1) (mg C m^{-3}) seasonal cycles. Colours refer to (A) diatom molar C:P; (B) diatom molar C:N ratios; (C) microzooplankton (Z1) assimilation efficiency (Zeff) and (D) grazing (Z1 over P1, mg C m^{-3} d^{-1}).

Fig 5. Scatter plots of modelled diatom (P1) biomass (mg C m^{-3}) and carbon to nutrient molar ratios. Colour scales indicate: (A) and (B) microzooplankton (Z1) assimilation efficiency (Zeff); (C) and (D) grazing (Z1 over P1, mg C m^{-3} d^{-1}). Simulations refer to daily averaged surface values for the period 2000-2009

Fig. 6. (A) simulated Z1-P1 predator-prey system (biomasses and grazing) and (B) specific carbon exudation rate subsampled from the modelled time series. Biomass is given in mg C m^{-3}, grazing in mg C m^{-3} d^{-1} and the carbon specific exudation rate in d^{-1}. Colours refer to diatom molar C:P.

Fig. 7. Simulated diatom (P1) and microzooplankton (Z1) seasonal cycle as in Fig. 4, but with reduced (by 50%) nitrate and phosphate as initial conditions.

Fig. 8. Scatter plots as in Fig. 5 but with reduced nitrate and phosphate concentration as initial condition. Nutrient concentrations were reduced by 50%.

Fig. 9. Climatological (2000-2009) diatom (P1) and microzooplankton (Z1) monthly averaged seasonal cycles simulated with the standard ERSEM formulation. Colours refer to: (A) C:P diatom molar ratio; (B) C:N diatom molar ratios and (C) grazing (Z1 over P1, mg C m^{-3} d^{-1}).

Fig. 10. Simulated diatom (P1) and micrzooplankton (Z1) seasonal cycle as in Fig 8 but with reduced (by 50%) nitrate and phosphate initial conditions.

Fig. 11. Monthly averaged, diatoms (P1) and microzooplankton (Z1) biomass (mg C m^{-3}) simulated in the sensitivity experiments described in Table 3.

Fig. 12. Conceptual model describing the formation and evolution of a diatom bloom. Biotic processes are highlighted in blue. Red arrows imply the action of physical forcing such as NHF, TKE and MLD.

Fig. 13. Scatter plot ($r=0.8$, $p<0.001$) between simulated diatom (P1) carbon to phosphorus ratio (mol mol^{-1}) and NHF (W m^{-2}). Colorbar refers to microzooplankton (Z1) assimilation efficiency (Zeff).

REFERENCES

Atkinson, A., Harmer, R.A., Widdicombe, C.E. McEvoy, A.J., Smyth, T.J., Cummings, D.G., Somerfield, P.J., Maud, J.L. McConville, K. (in review) Questioning the role of phenology shifts and trophic mismatching in a planktonic food web.

Baretta, J.W., Ebenhoh, W. and Ruardij, P., 1995. The European regional Seas Ecosystem Model, a complex marine ecosystem model. Neth. J. Sea Res., 33, 233–246

Bautista, B., Harris, R.P., 1992. Copepod gut contents, ingestion rates and grazing impact on phytoplankton in relation to size structure of zooplankton and phytoplankton during a spring bloom. Mar. Ecol. Prog. Ser. 82, 41-50.

Blackford, J. C., Allen, J. I., Gilbert, F. J., 2004. Ecosystem dynamics at six contrasting sites: a generic modelling study. J. Mar. Syst., **52**,191-215.

Branco, P., Stomp, M., Egas, M., Huisman J., 2010. Evolution of nutrient uptake reveals a trade-off in the ecological stoichiometry of plant herbivore interactions. Am. Nat., 176, 162-176

Burchard, H., Bolding, K., Villareal, M. 1999 GOTM: a general ocean turbulence model. Theory, applications and test cases. Technical Report EUR 18745 EN, European Commission

Calbet, A., Landry, M. R., 2004. Phytoplankton growth, microzooplankton grazing, and carbon cycling in marine systems. Limnology and Oceanography; 49:51-57.

Diehl, S., 2007. Paradoxes of enrichment: Effects of increased light versus nutrient supply on pelagic producer–grazer systems. American Naturalist 169, E173–E191.

Ebenhoh, W., Baretta, J.W., Baretta-Bekker, J.G., 1997. The primary production model in a marine ecosystem model ERSEM II. Journal of Sea Research 38, 169–172.

Elser, J.J., Loladze, I., Peace, A.L., Kuang, Y., 2012. Lotka re-loaded: modelling trophic interactions under stoichiometric constrains. Ecological Modelling 245, 3-11

Flynn, K.J., Davidson, K., Cunningham, A., 1996. Prey selection and rejection by amicroflagellate; implications for the study and operation of microbial food webs. J. Exp. Mar. Biol. Ecol. 196, 357-372

Flynn, K. J., Davidson, K., 1993. Predator–prey interactions between Isochrysis galbana and Oxyrrhis marina. II. Release of non-protein amines and faeces during predation of Isochrysis. J. Plankton Res., 15, 893–905.

Geider, R. J., MacIntyre, H. L., Kana, T. M., 1997. Dynamic model of phytoplankton growth and acclimation: responses of the balanced growth rate and the chlorophyll a:carbon ratio to light, nutrient-limitation and temperature. Mar. Ecol. Prog. Ser. 148, 187-200

Geider, R., La Roche, J., 2002. Redfield revisited: variability of C:N:P in marine microalgae and its biochemical basis. European Journal of Phycology 37, 1-17

Hall, S.R., 2004. Stoichiometrically-explicit competition between grazers: species replacement, coexistence, and priority effects along resource supply gradients. American Naturalist 164, 157–172.

Huisman, J., van Oostveen, P., Weissing, F.J., 1999. Critical depth and critical turbulence: Two different mechanisms for the development of phytoplankton blooms. Limnology and Oceanography 44: 1781-1787

Hessen, O.D., Faerovig, J.P., Andersen, T., 2002. Light, nutrients, and P:C ratios in algae: grazer performance related to food quality and quantity. Ecology 83, 1886-1898

Irigoien, X., Flynn K.J., Harris, R.P., 2005. Phytoplankton blooms: a 'loophole' in microzooplankton grazing impact? J. Plankton Res. 27, 313-321

Jones, R.H, Flynn, K.J., 2005. Nutritional status and diet composition affect the value of diatoms as copepod prey. Science 307, 1457-14-59

Kiørboe, T., 2008. A mechanistic approach to plankton ecology. Princeton University Press, 209 pp

Kondo, J., 1975. Air-sea bulk transfer coefficients in adiabatic conditions. Boundary-Layer Meteorol., 9, 91–112.

Kovala, P. E., Larrance, J. D., 1966. Computation of phytoplankton cell numbers, cell volume, cell surface and plasma volume per liter, from microscopical counts. DTIC Document.

Legendre, L., 1990. The significance of microalgal blooms for fisheries and for the export of particulate organic carbon in oceans. J. Plankton Res. 12, 681-699

Loladze, I., Kuang, Y., Elser, J.J., 2000. Stoichiometry in producer-Grazer System: linking Energy Flow with Elemental Cycling. *Bulletin of Mathematical Biology*, 62: 1137-1162.

Loladze, I., Kuang, Y., Elser, J.J., Fagan, W.F., 2004. Competition and stoichiometry: coexistence of two predators on one prey. Journal of Theoretical Biology 65, 1–15

Martiny, A. C., Vrugt, J.A., Primeau, F.W., Lomas M.W., 2013. Regional variation in the particulate organic carbon to nitrogen ratio in the surface ocean. Global Biogeochem. Cycles, 27, 723–731, doi:10.1002/gbc.20061.

Menden-Deuer, S., Lessard, E. J., 2000. Carbon to volume relationships for dinoflagellates, diatoms, and other protist plankton. Limnology and oceanography, 45, 569-579.

Mitra, A., 2006. A multi-nutrient model for the description of the stoichiometric modulation of predation in micro- and mesozooplankton. J. Plankton. Res. 28, 597-611

Mitra, A., Flynn, K.J., 2006. Promotion of harmful algal blooms by zooplankton predatory activity. Biology Letters 2, 294-197

Mitra, A, Flynn, K.J., 2007. Effects of food quality and quantity on consumer gut passage time; impacts on predation kinetics and trophic dynamics. Am. Nat. 169:632-646.

Mitra, A., Castellani, C., Gentleman, W., Jónasdóttir, S.H., Flynn, K.J., Bode, A., Halsband, C., Kuhn, P., Licandro, P., Agersted, M.D., Calbet, A., Lindeque, P., Koppelmann, R., Møller, E.F., Gislason, A., Nielsen, T.G., St. John, M., 2014. Bridging the gap between marine biogeochemical and fisheries sciences; configuring the zooplankton link. Prog. Oceanogr., in press. http://dx.doi.org/10.1016/j.pocean.2014.04.025.

Pastres, R., Ciavatta, S., 2005. A comparison between the uncertainties in model parameters and in forcing functions: its application to a 3D water-quality model. *Environmental Modelling & Software*, *20*(8), 981-989.

Polimene, L., Brunet, C., Butenschon, Martinez-Vicente, V., M., Widdicombe, C., Torres, R., Allen, J.I.,. 2014. Modelling a light-driven phytoplankton succession. J. Plankton Res. 36, 214-229

Polovina, J. J., Howell, E. A., Abecassis, M., 2008. Ocean's least productive waters are expanding, Geophys. Res. Lett., 35, L03618, doi:10.1029/2007GL031745.

Rosati, A., Miyakoda, K., 1988. A general circulation model for upper ocean simulation. J. Phys. Oceanogr., 18, 1601–1626.

Sailley, S.F.,Vogt, M., Doney, S.C., Aita, M.N., Bopp, L., Buitenhuis, E.T., Hashioka, T., Lima, I., Le Quere, C., Yamanaka, Y., 2013. Comparing food web structures and dynamics across a suite of marine ecosystem models. Ecological Modelling. 261-262, 43-57

Saltelli, A., K. Chan, and M. Scott (Eds.) (2000). *Sensitivity Analysis*. Wiley Series in Probability and Statistics. New York: John Wiley and Sons.

Sarmiento, J.L., Gruber, N., 2006. Ocean Biogeochemical Dynamics. Princeton University Press

Siuda, N.S.A., Dam, G.H., 2010. Effects of omnivory and predator-prey elemental stoichiometry on planktonic trophic interactions. Limnol. Oceanogr. 55, 2107-2116

Smyth, T. J., Fishwick, J. R., Al-Moosawi, L., Cummings, D.G., Harris, C., Kitidis, V., Rees, A., Martinez-Vicente, V., Woodwaed, E.M.S., 2010. L4 in context: a broad spatio-temporal view in the Western English Channel Observatory. J. Plankton Res., **32**, 585–601

Smyth, T.J., Allen, I., Atkinson, A., Bruun, J.T., Harmer, R.A., Pingree, R.D., Widdicombe C.E., Somerfield, P.J., 2014. Ocean Net Heat Flux Influences Seasonal to Interannual Patterns of Plankton Abundance. PLoS ONE 9(6): e98709. doi:10.1371/journal.pone.0098709

Stiefs, D., van Voorn, G.A.K., Kooi, B.W., Feudel, U., Gross, T., 2010. Food quality in producer–grazer models: a generalized analysis. American Naturalist, 176367–176380.

Taylor, J.R., Ferrari, R., 2011. Shutdown of turbulent convection as a new criterion for the onset of springphytoplankton blooms. Limnology and Oceanography 56: 2293-2307.

Urabe, J., Sterner, W.R., 1996. Regulation of herbivore growth by the balance of light and nutrients. Proc. Natl. Acad. Sci. 93, 8465-8469

Vichi, M., Masina, M.,Pinardi, N., 2007. A generalized model of pelagic biogeochemistry for the global ocean ecosystem. Part I: Theory. J. Mar. Sys. 64, 89–109.

Widdicombe, C.E., Eloire, D., Harbour, D. Harris, R.P., Somerfield, P.J., 2010. Long-term phytoplankton community dynamics in the Western English Channel. J.Plankton Res. 32, 643-655.

Woodward, E.M.S., Harris, C., Al-Moosawi, L., 2013. Nutrient concentration profiles from long term time series at Station L4 in the Western English Channel from 2000 to 2012. British Oceanographic Data Centre - Natural Environment Research Council UK. doi:10.5285/075f8000-7114-11e2-907f-1803734a77fb

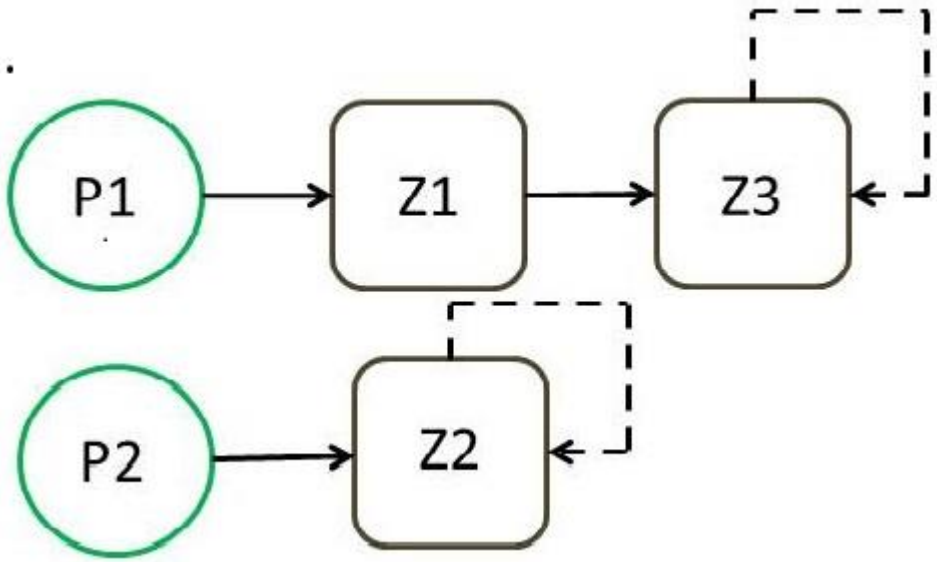

Fig 1

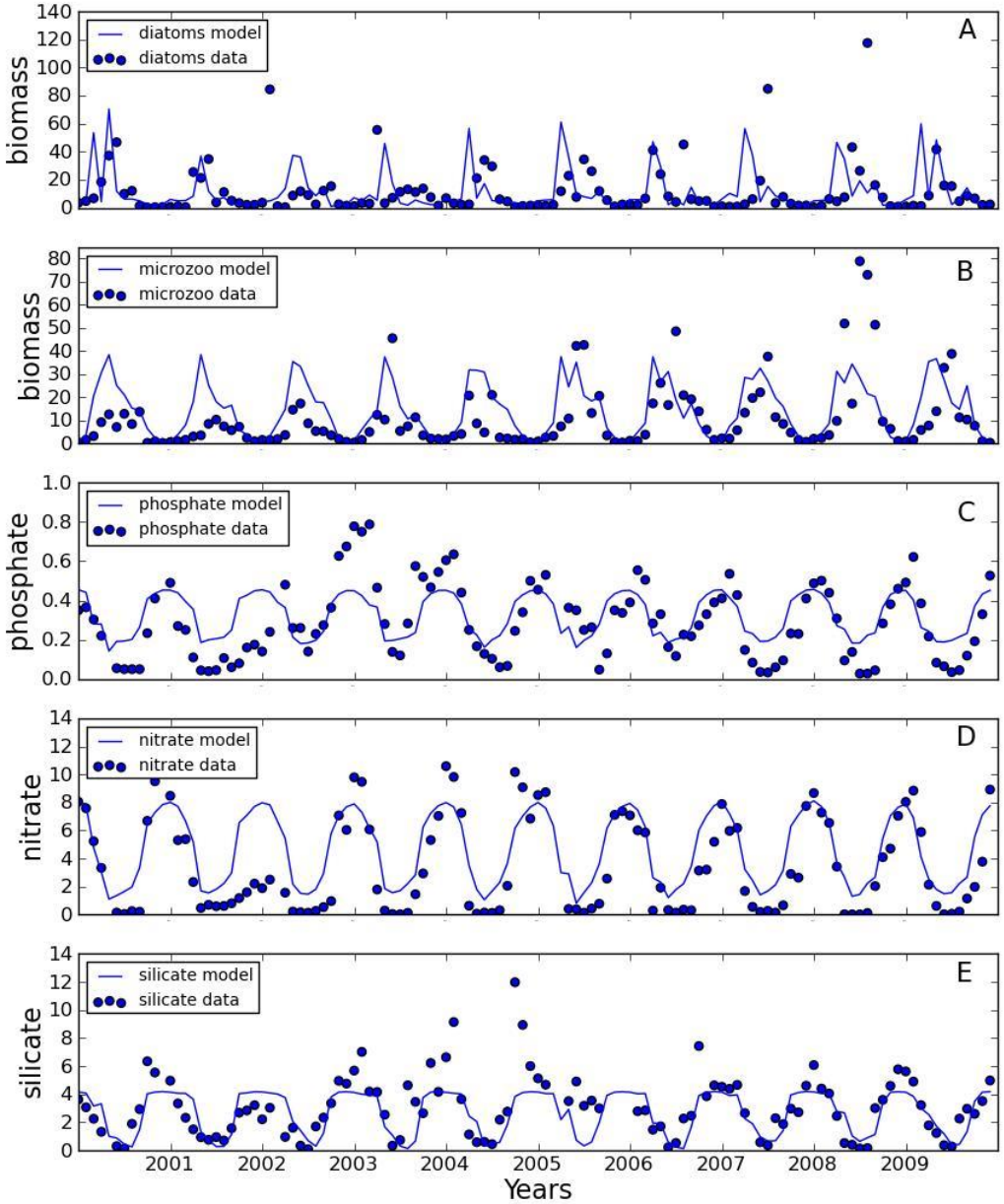
A
diatoms model
diatoms data
biomass
B
microzoo model
microzoo data
biomass
C
phosphate model
phosphate data
phosphate
D
nitrate model
nitrate data
nitrate
E
silicate model
silicate data
silicate
2001
2002
2003
2004
2005
2006
2007
2008
2009
Years

Fig 2

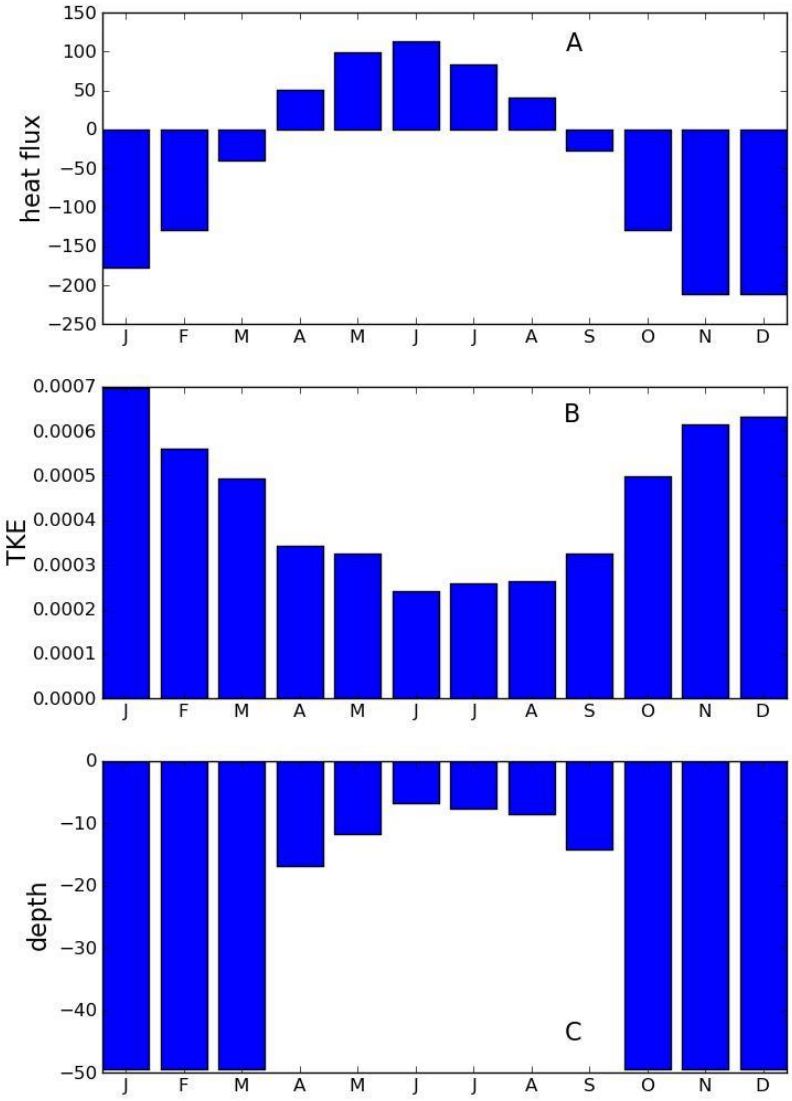
A
heat flux
150
100
50
0
−50
−100
−150
−200
−250
J F M A M J J A S O N D
B
TKE
0.0007
0.0006
0.0005
0.0004
0.0003
0.0002
0.0001
0.0000
J F M A M J J A S O N D
C
depth
0
−10
−20
−30
−40
−50
J F M A M J J A S O N D

Fig 3

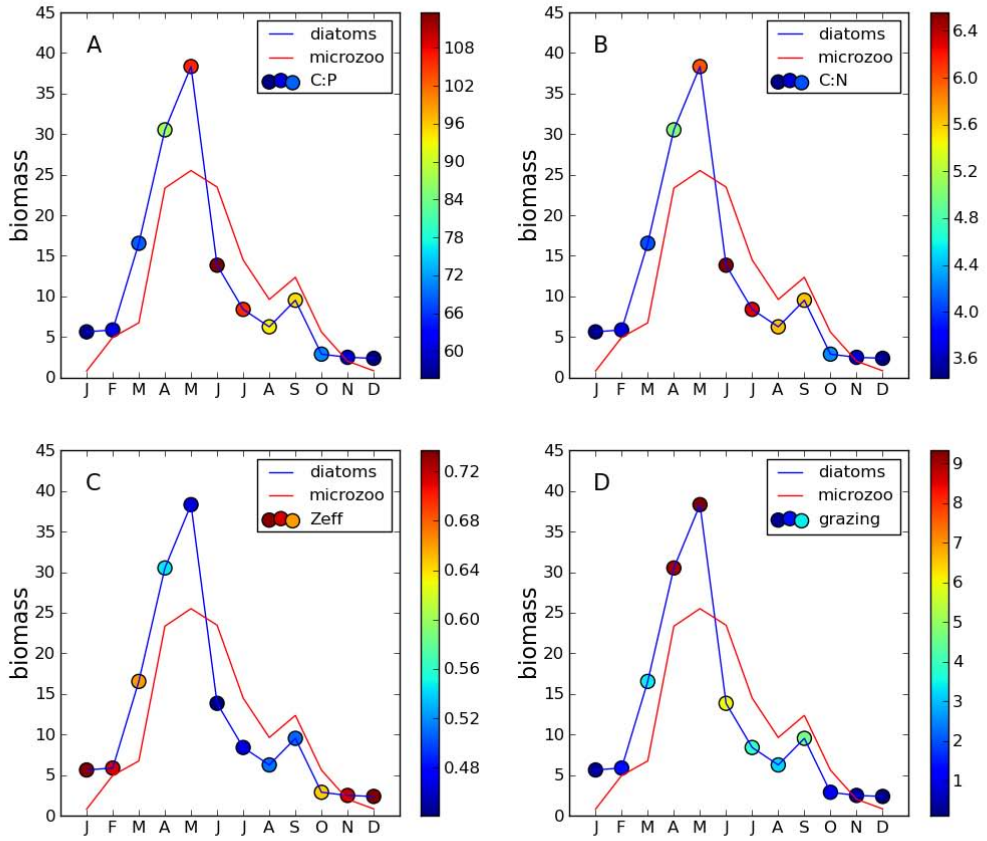
A
diatoms
microzoo
C:P
B
diatoms
microzoo
C:N
C
diatoms
microzoo
Zeff
D
diatoms
microzoo
grazing
biomass
J F M A M J J A S O N D

Fig 4

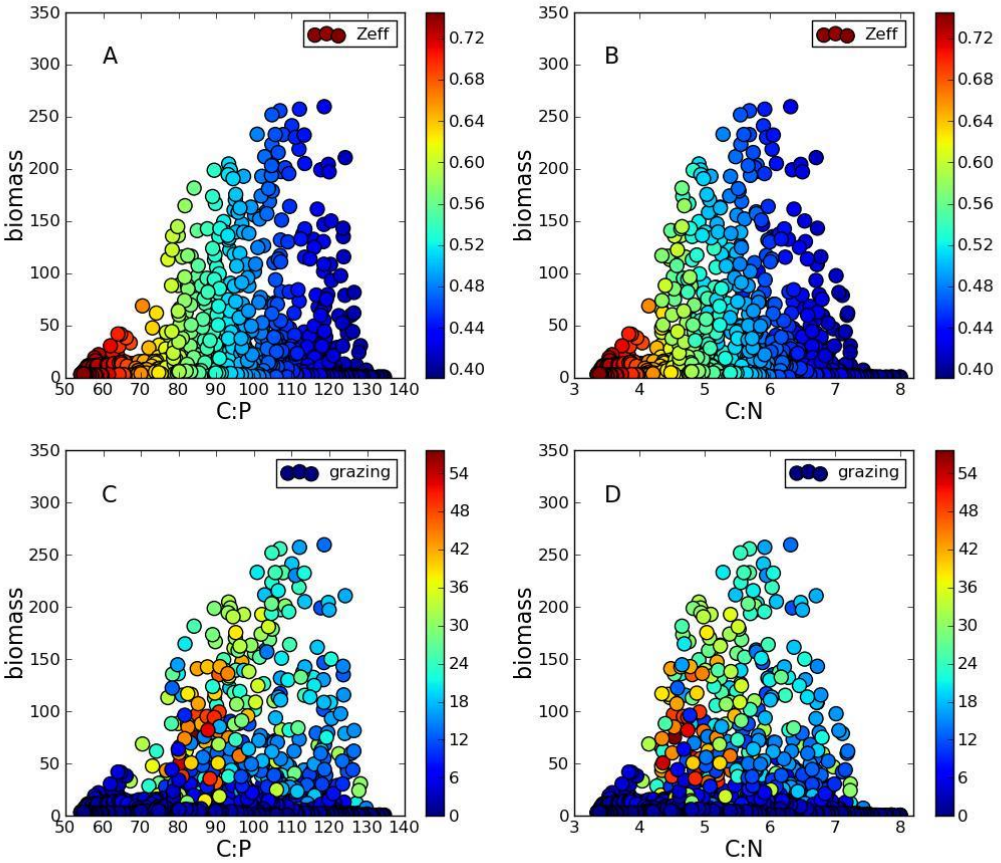

Fig 5

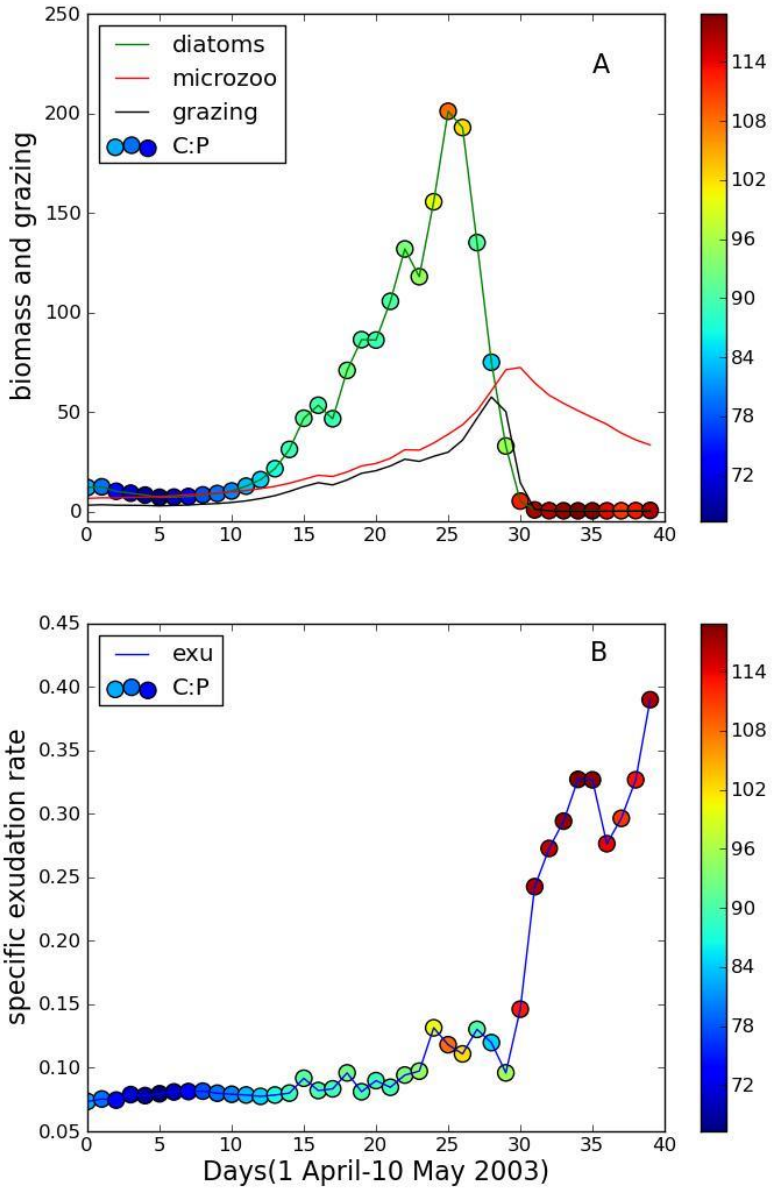
A
diatoms
microzoo
grazing
C:P
biomass and grazing
B
exu
C:P
specific exudation rate
Days(1 April-10 May 2003)

Fig 6

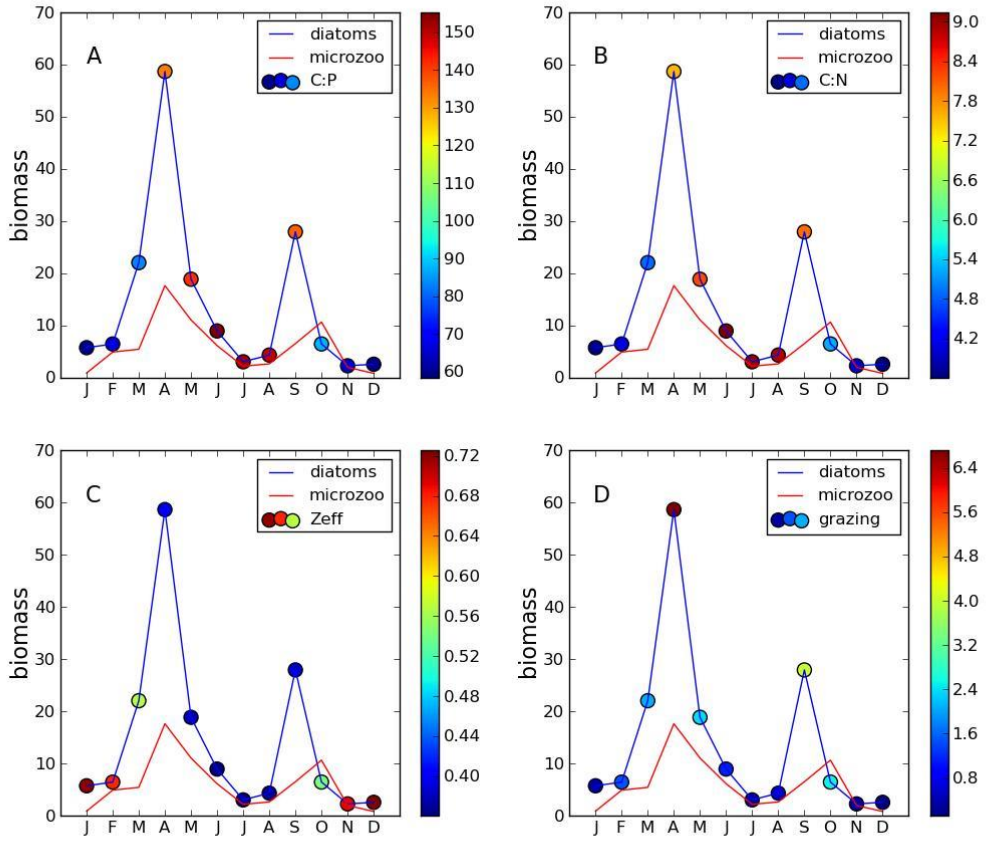
A
diatoms
microzoo
C:P
B
diatoms
microzoo
C:N
C
diatoms
microzoo
Zeff
D
diatoms
microzoo
grazing
biomass
J F M A M J J A S O N D

Fig 7

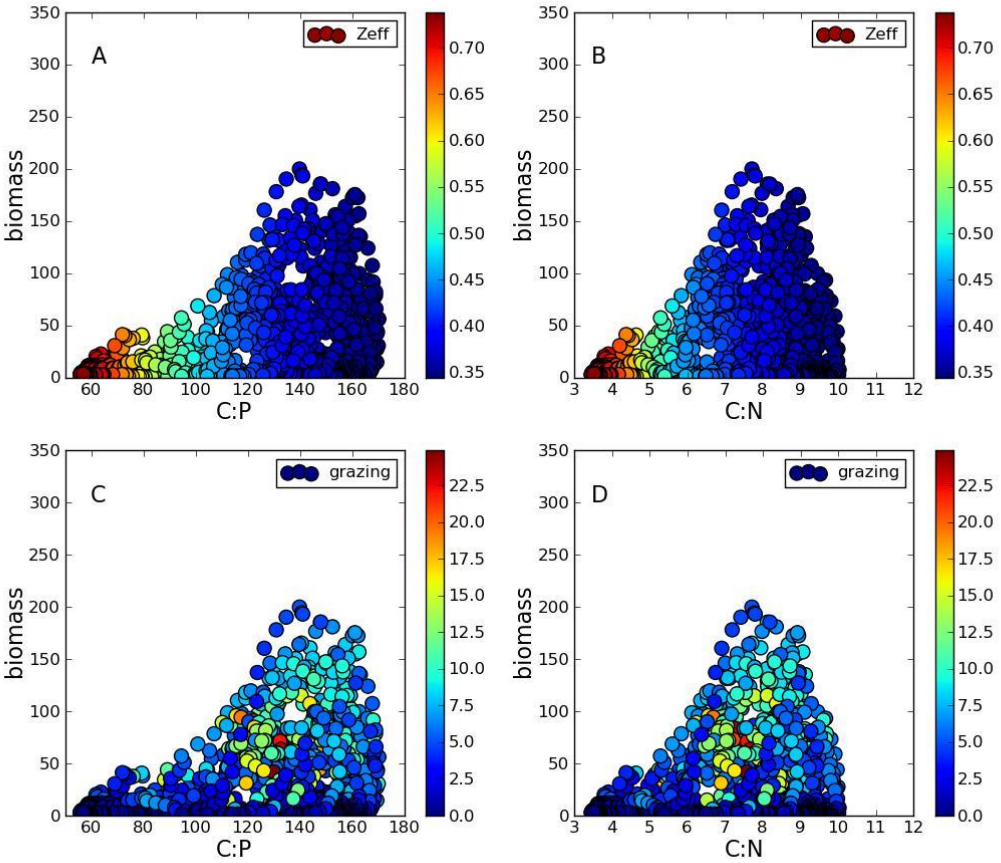

Fig 8

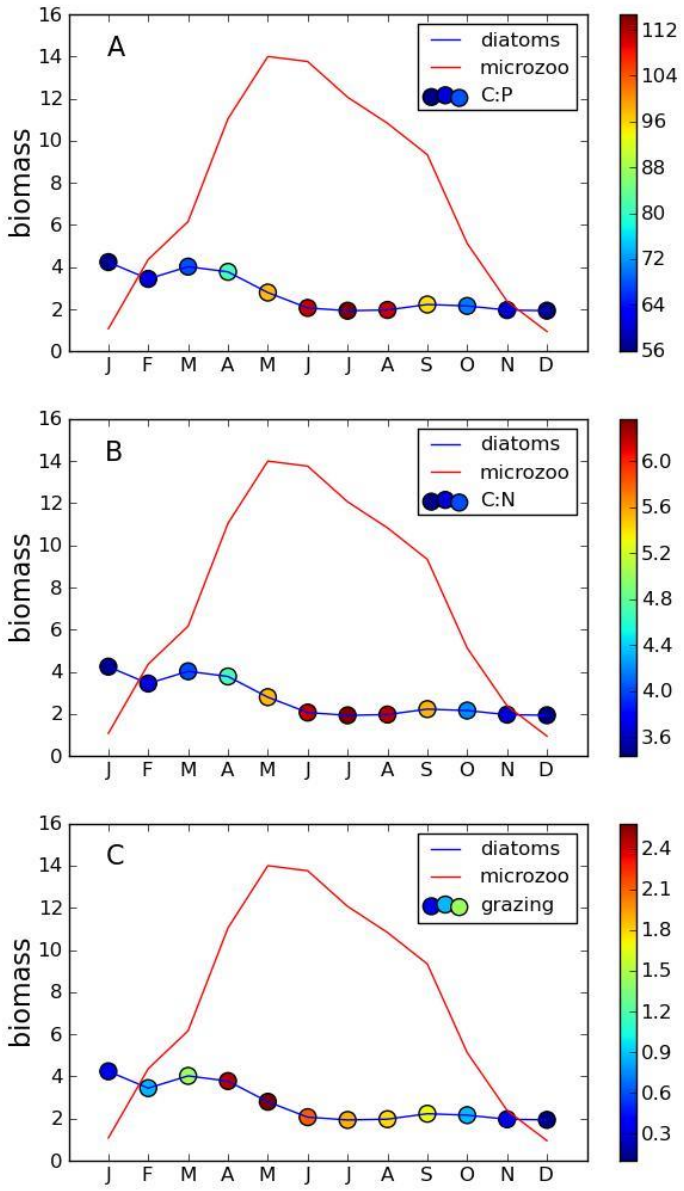
A
diatoms
microzoo
C:P
biomass
B
diatoms
microzoo
C:N
biomass
C
diatoms
microzoo
grazing
biomass
J F M A M J J A S O N D

Fig 9

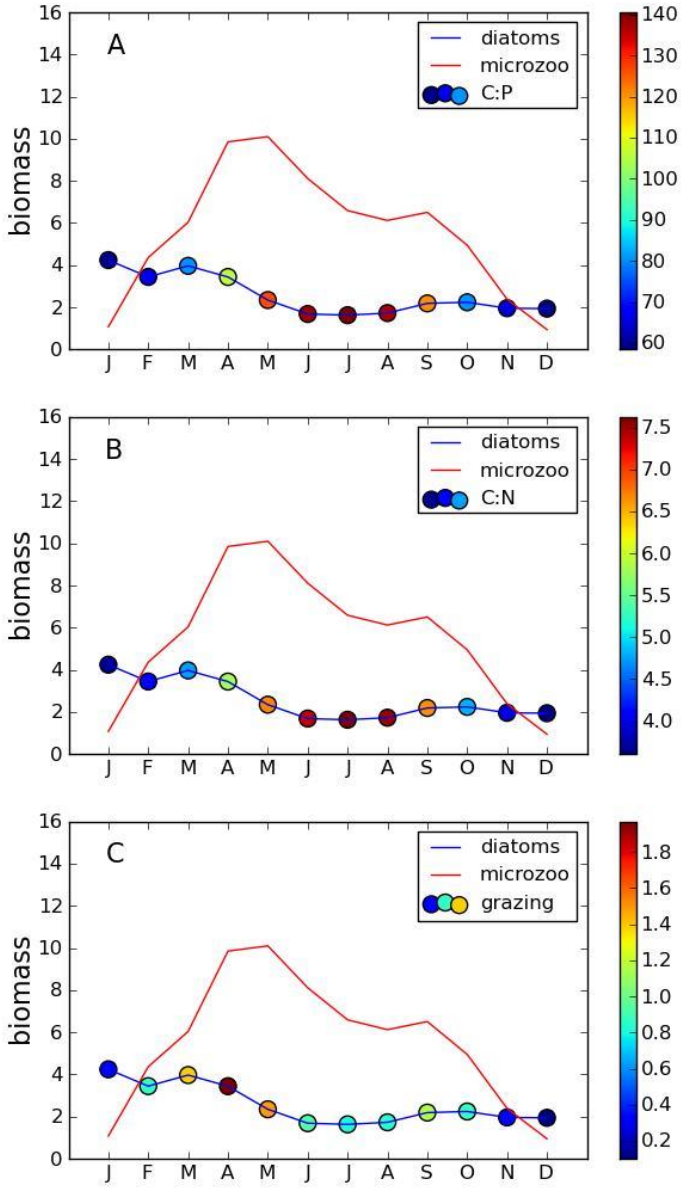
A
diatoms
microzoo
C:P
biomass
B
diatoms
microzoo
C:N
biomass
C
diatoms
microzoo
grazing
biomass
J F M A M J J A S O N D

Fig 10

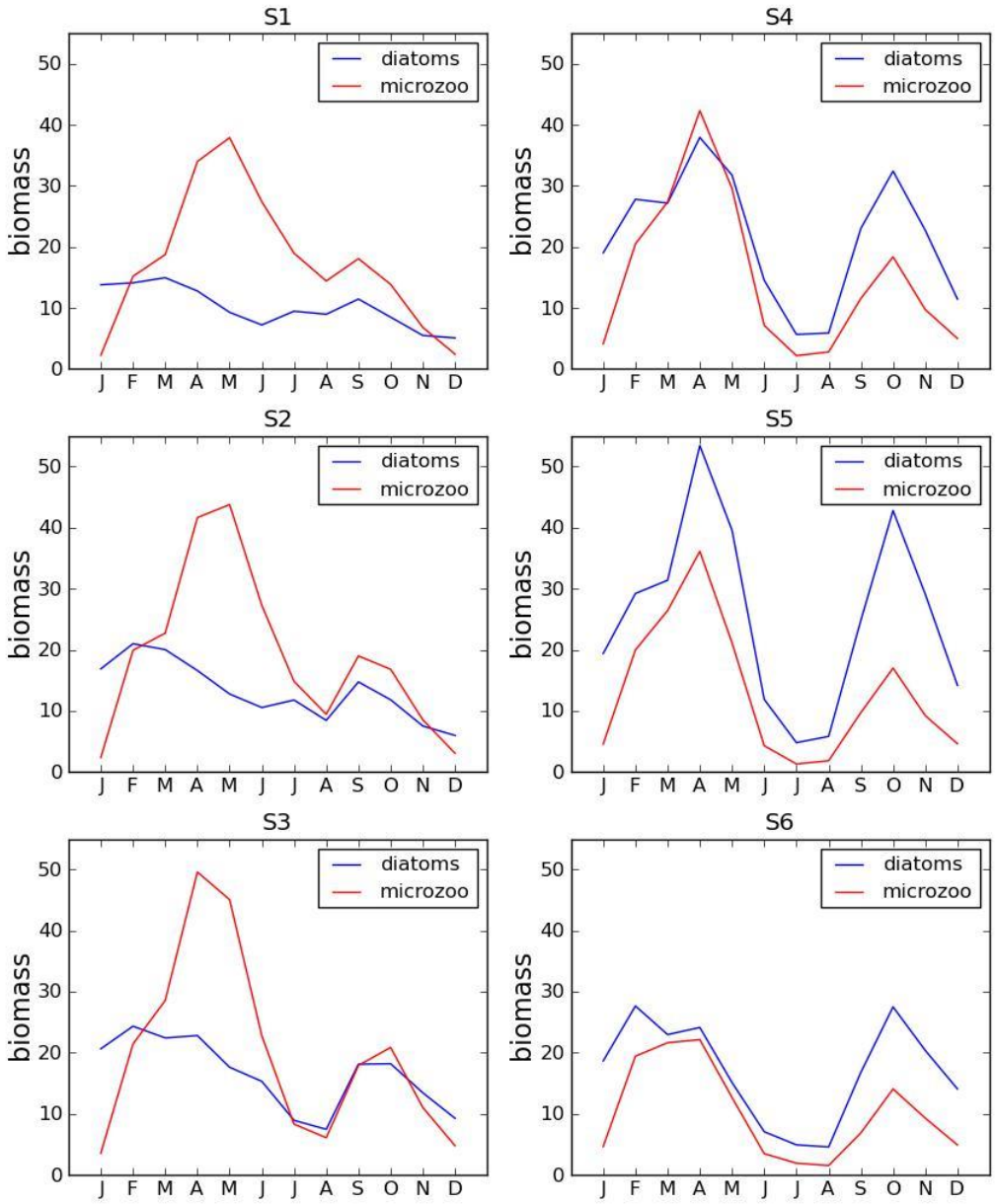
S1
S4
S2
S5
S3
S6
diatoms
microzoo
biomass
0
10
20
30
40
50
J F M A M J J A S O N D

Fig 11

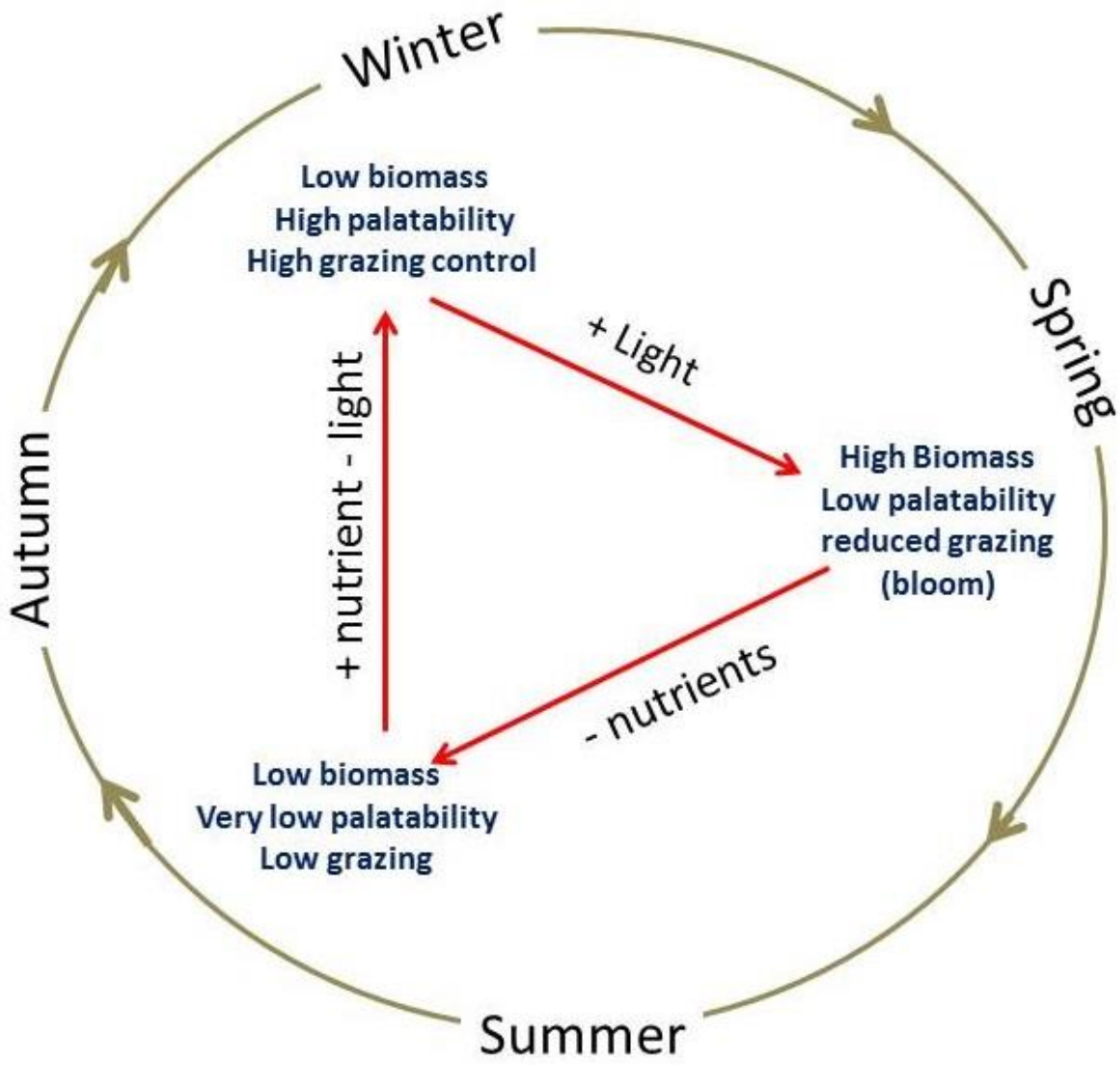
Winter
Spring
Summer
Autumn
Low biomass
High palatability
High grazing control
+ Light
High Biomass
Low palatability
reduced grazing
(bloom)
- nutrients
Low biomass
Very low palatability
Low grazing
+ nutrient - light

Fig 12

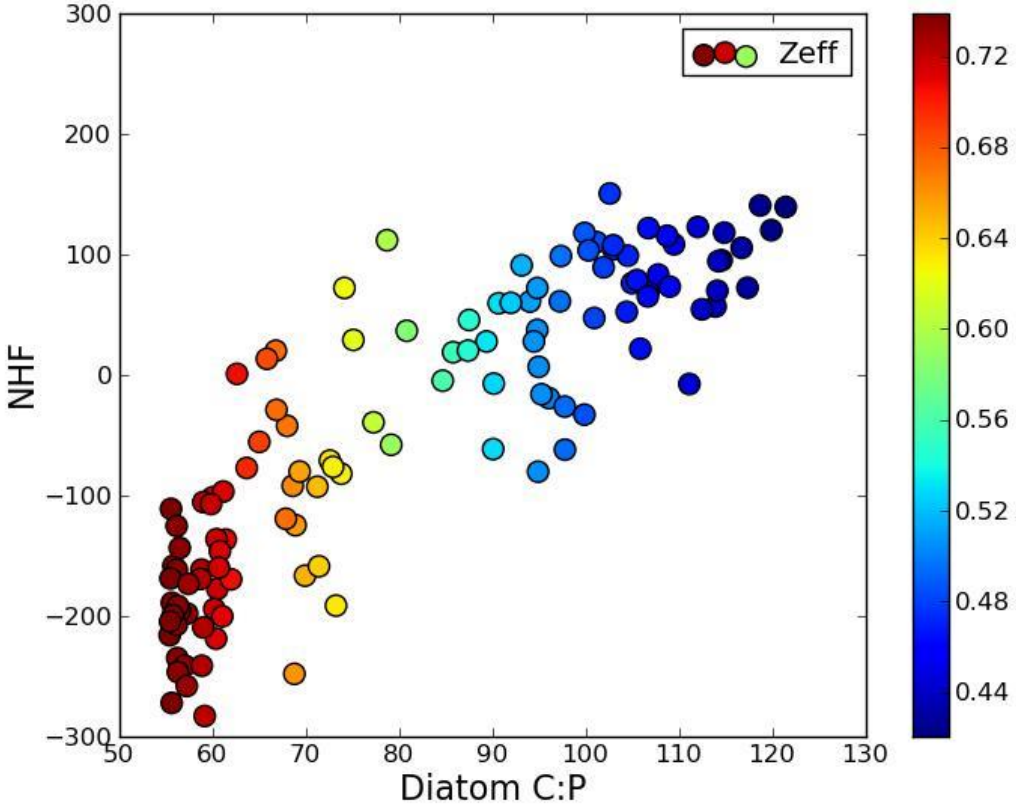
Zeff
NHF
Diatom C:P
300
200
100
0
−100
−200
−300
50
60
70
80
90
100
110
120
130
0.72
0.68
0.64
0.60
0.56
0.52
0.48
0.44

Fig 13